Original Research Article

Temporal lobe microstructural abnormalities in patients with nasopharyngeal carcinoma quantitatively evaluated by high-resolution DWI and DKI after concurrent chemoradiotherapy

Gang Wu [a,1], Rui-rui Li [b,1], Priya S. Balasubramanian [e], Meng-meng Li [c], Kai Yang [b], Wei-yuan Huang [b,d,*], Feng Chen [b,*]

[a] Department of Radiation Oncology, Hainan General Hospital (Hainan Affiliated Hospital of Hainan Medical University), Haikou, China
[b] Department of Radiology, Hainan Hospital of Hainan Medical College (Hainan General Hospital), Haikou, China
[c] Department of Research and Education, Hainan Hospital of Hainan Medical College (Hainan General Hospital), Haikou, China
[d] Department of Radiology, Weill Cornell Medical College, New York, NY, USA
[e] Department of Electrical and Computer Engineering, Cornell University, Ithaca, NY, USA

ARTICLE INFO

ABSTRACT

Purpose: To investigate temporal lobe microstructural abnormalities and neurocognitive function impairment after concurrent chemoradiotherapy (CCRT) in patients with nasopharyngeal carcinoma (NPC).
Methods: NPC patients who underwent CCRT were enrolled. High-resolution diffusion-weighted imaging (DWI) magnetic resonance imaging (MRI) and diffusion-kurtosis imaging (DKI) MRI, were performed 5 times per patient (once pre-CCRT, 1 week post-CCRT, 3 months post-CCRT, 6 months post-CCRT, and 12 months post-CCRT). Neurocognitive function was evaluated by Montreal Neurocognitive Assessment (MoCA) twice per patient, once pre-CCRT, and once 12-months after CCRT.
Results: Of 111 patients, 56 completed the entire protocol. The MRI derived apparent diffusion coefficient (ADC), mean of diffusion coefficient (Dmean) and fractional anisotropy (FA) values were significantly decreased ($p < 0.05$) over the 0–3 month period following CCRT and significantly increased ($p < 0.05$) over the 3–12 month period following CCRT. The mean of kurtosis coefficient (Kmean) continued to decline over a year post-CCRT. All parameters reveal more pronounced changes in white matter (WM) than in grey matter (GM). MoCA also declined after CCRT ($p < 0.001$). MoCA showed significant positive correlation with Kmean-WM-6 m, Kmean-WM-12 m and ΔKmean-WM.
Conclusions: High-resolution DWI and DKI should be considered as a promising method for the investigation of temporal lobe microstructural change in NPC patients after CCRT.

1. Background

Temporal lobe necrosis or injury is one of the severe complications of nasopharyngeal carcinoma (NPC) after radiotherapy (RT) (+/− chemotherapy) due to the nonlocalized nature of the RT and sensitivity of nervous tissue to RT [1]. The 3- and 5-year incidences of conventional two-dimensional RT-induced temporal lobe necrosis have been reported to be 10.8% and 34.9%, respectively [2].

With the increasing application of intensity-modulated radiotherapy (IMRT), the incidence significantly decreased to 5% [3]. IMRT enables the delivery of the prescribed RT dose to the planning target volumes (PTV), and allows for the reduction the dose for organs at danger, such as the temporal lobe, brainstem, and optic chiasm [4]. The IMRT technology is able to create precision delivery of dosage to tumors by using beam collimation techniques (Multileaf Collimators) and feedback controlled intensity distribution through computation [5]. This allows for a localized delivery of RT that influences surrounding, nontarget tissue less. However, NPC survivors treated with IMRT (+/− chemotherapy) are still at significant risk of both neurocognitive and neurobehavioral impairment symptoms, including headaches, memory loss, anxiety, depression, communication or behavioral changes, etc. Previous researchers have performed clinical series studies that have

---

* Corresponding authors at: Department of Radiology, Hainan General Hospital (Hainan Hospital of Hainan Medical College), No. 19 Xiuhua St Xiuying DIC, Haikou, Hainan 570311, China (W. Huang).
E-mail addresses: weh4001@med.cornell.edu (W.-y. Huang), fenger0802@163.com (F. Chen).
[1] The authors Gang Wu and Rui-rui Li contributed equally to this work.

assessed neurocognitive function in head and neck cancer patients. One particular cross-sectional study demonstrated that 32% NPC patients have impaired Montreal Neurocognitive Assessment (MoCA) scores with a median follow-up of 7.5 years after the completion of IMRT [6]. Another study found that longitudinal assessment of NPC patients present with neurocognitive test scores that progressively decline in the 2 years following chemotherapy or radiation administration [7]. The neurocognitive function scores are affected by many factors rather than treatment only. Previous studies cite that disease status or communication difficulty after RT influence the neurocognitive function and quality of life in head and neck cancer survivors [8,9]. While it is clear that neurocognitive function scores are and will remain a hallmark in patient evaluation, there is a clear difficulty in identifying and decoupling factors that may influence the more qualitative patient scoring methods. This provides a motivation to develop quantitative parameters that allow for clinicians and researchers to evaluate patients undergoing RT for NPC in a more rigorous manner.

Given that macro/micro-structural changes in the brain underlie neurocognitive impairment, this research study is motivated by the hypothesis that MRI deduced micro and macrostructural changes can provide insights on detecting temporal lobe injury in RT treated NPC patients more sensitively than the established neurocognitive score. There are three phases of the pathophysiological reaction to irradiation in normal brain tissue: the acute reaction period (few days to few weeks), early delayed radiation period (1–6 months), and late delayed radiation period (6 months to few years) [10,11]. Lv et al. [12] found that time-dependent volumetric decreases for the total gray matter (GM) of the bilateral temporal lobe, as well as time-dependent ventricle expansion in NPC patients through acute reaction period to delay radiation period. Wang et al. [13] reported that bilateral temporal white matter (WM) microstructural changes following RT is dependent on the duration of completion of radiotherapy. RT-induced microstructural injury and multiple sclerosis in normal-appearing temporal lobes have been confirmed through the use of in-vivo model studies by analyzing tissue ex-vivo using histopathology staining techniques [14,15]. The aforementioned research suggest that temporal lobes that may appear healthy with conventional magnetic resonance imaging (MRI) could have microstructural abnormalities in both GM and WM, and this must be confirmed using different techniques aside from conventional MRI. In order to obtain a quantitative measure to understand micro and macro structural changes in NPC patients undergoing RT, a technique other that conventional MRI must be utilized.

Conventional MRI has limited power in detecting microstructural injury of the temporal lobe. In comparison, diffusion-weighted imaging (DWI), diffusion-tensor imaging (DTI), and diffusion-kurtosis imaging (DKI) are diagnostic and research techniques that enable examination of tissue microcirculation and biophysical properties by exploiting the information from Brownian motion of water molecules in biological tissues [16]. DWI and DTI have been applied in NPC to detect radiation-induced temporal WM damage that is not visible using conventional imaging modalities [17,18] As a non-Gaussian model technique, DKI specifically reflects both complex diffusion and kurtosis alterations by utilizing the distributional properties of the tissue compartments in GM or WM [19], as recently shown in other cross-sectional studies [20]. Given that DWI and DKI are sensitized to the diffusion of water and the restriction of water diffusion, changes in these parameters could indicate potential edema, ischemic necrosis, and even progressive vascular remodeling, in addition to tissue remodeling [16]. Identifying whether these functional imaging techniques (DWI and DKI) could detect microstructural injury in NPC patients treated by chemoradiotherapy would important for implications of early intervention and improvement of quality of life.

Herein, with 56 analyzable NPC patients, we present our prospective longitudinal study providing an evaluation of microstructural temporal lobe abnormalities by MRI parameter changes, and neurocognitive function changes after concurrent chemoradiotherapy (CCRT).

2. Methods

2.1. Patient selection

NPC patients who were diagnosed by nasopharyngoscopic needle biopsy and participated CCRT in the Department of Radiation Oncology, Hainan General Hospital (Affiliated Hainan Hospital of Hainan Medical College) between September 2015 and May 2018 were enrolled. Patients met inclusion criteria by (1) having Karnofsky performance status ≥70%, (2) undergoing each MRI follow-up in our hospital, and (3) having no imaging evidence of tumor invading the temporal lobes or temporal necrosis. Patients were excluded who had (1) MRI (eg, artificial cochlea, cardiac pacemaker implantation) or CCRT contraindications, (2) suffered from other neurological or psychiatric diseases, (3) had previously received radiotherapy in the neck region, (4) had brain metastases or trauma, and (5) a baseline MoCA score <25. The study was approved by the Ethics Committee of Hainan General Hospital, and all patients provided written informed consent.

2.2. Follow-up procedure

To assess early CCRT-related brain microstructural alterations (from acute reaction period, early delayed radiation period, to late delayed radiation period), NPC patients were evaluated at the following time points: before initiation of treatment (baseline), within 1 week, 3 months, 6 months, and 12 months after the completion of CCRT treatment. At each time point, nasopharynx and/or neck MRI (DWI and DKI) was performed. Neurocognitive testing of MoCA was performed at the first and last time points (MoCA-pre, MoCA-post). Fig. 1 illustrates the flow chart of the participant selection procedure.

2.3. MRI protocol

MRI was performed using a 3T MR scanner (Skyro, Siemens Healthcare, Erlangen, Germany) with a 20-channel head/neck coil. The protocol included axial proton density-weighted images (PdWI), axial pre- and post-gadolinium T1-weighted images (T1WI) (Gd-DTPA: 0.1 mmol/kg), high-resolution DWI and DKI. PdWI and TIWI were utilized as conventional protocols to extract head and neck anatomical structure information, and high-resolution DWI and DKI were utilized as diffusion sequences to provide quantitative diffusion parameters for the tissue of interest. PdWI scanning was acquired at a repetition time (TR) of 5200 ms, echo time (TE) of 20 ms, 220 * 220 mm^2 field of view (FOV), and 4.0 mm slice thickness. High-resolution DWI scanning was acquired using a readout segmentation of long variable echo-trains diffusion weighted imaging (RESOLVE) sequence at a TR of 5800 ms, TE of 68 ms, 220 * 220 mm^2 FOV, 1.3 * 1.3 * 4 mm^2 voxel size, and 4.0 mm slice thickness. The DWI sequence was carried out using b values of 0 and 1000 s/mm^2 in three different directions. DKI scanning was acquired at a TR of 7700 ms, TE of 88 ms, 220 × 220 mm^2 FOV, 2.5 × 2.5 × 4 mm^2 voxel size, and 4.0 mm slice thickness. The DKI sequence was carried out using b values of 0, 500, 1000, and 1500 s/mm^2 in 30 different gradient encoding directions.

Post-processing of raw DKI data was performed using the Diffusional Kurtosis Estimator (DKE, version 2.6, built on February 25,
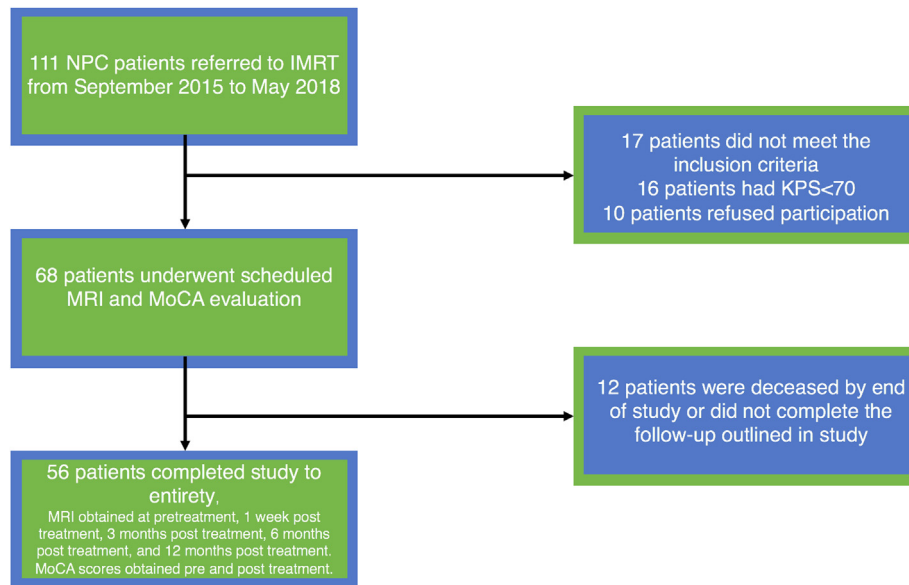
Fig. 1. Flow chart of participant selection procedure.

2015) software [21]. The ADC map was derived from high-resolution DWI using software provided by the manufacturer of Siemens (Syngo.via). The parameters (-pre, -post, -3 m, -6 m, -12 m) were measured and reported using the software "ITK-SNAP" (version 3.4.0, http://www.itksnap.org) [22]. The regions of interest (ROIs) were delineated to obtain the temporal lobe GM and WM on both sides manually on axial images of the maximum hippocampal/hippocampus body level on the four parameters mappings and PdWI (automatic synchronized three-dimensional positioning) by clinical radiologist (R.-R. Li), eliminating the inclusion of the two sides of the middle cerebral artery, lateral ventricles, or obvious image derived artifacts (Fig. 2). All ROIs were confirmed by a senior radiologist (W.-Y. Huang)

2.4. Neurocognitive function evaluation

Neurocognitive function was assessed in the categories of visuospatial/executive, naming, memory, attention, language, abstraction, delayed recall and orientation by MoCA (Beijing Version) [23]. MoCA scores can range from 0 to 30 and the completion time of test was about 10 min. All patients completed this procedure under the supervision of medical professionals after receiving standardized and thorough explanation. Patients with <12 y of education receive a bonus point [24]. A score of <26 to define neurocognitive impairment, as supported by prior work [23,24].

2.5. Treatment protocol

All 56 patients presented with stage II-IV NPC according to the American Joint Committee on Cancer (AJCC 8th Edition) and received CCRT. Radiotherapy was carried out according to the institutional guidelines. IMRT planning was performed on the Eclipse Treatment Planning System (Major build version 11.0.47, USA) using the simultaneous integrated boost technique [25]. Target volumes were delineated slice-by-slice on treatment planning CT scans using an individualized delineation protocol that complied with International Commission on Radiation Units and Measurements reports 62 and 83, MRI for reference. The prescribed radiation dose was as follows: a total dose of 68.2–72.6 Gy in 31–33 fractions at 2.15–2.36 Gy/fraction to the planning target volume (PTV) of the GTVP, 60–70 Gy to the nodal gross tumor volume PTV (GTV-N), 60–65 Gy to the PTV of CTV-1 (high-risk regions), and 53–58 Gy to the PTV of CTV-2 (low-risk regions and neck nodal regions). All patients were treated with one fraction, daily, over five days per week. Concurrent chemotherapy protocol was chosen one of them: 1. Cisplatin (30–40 mg/m^2) weekly; 2. Cisplatin (80–100 mg/m^2) chemotherapy on days 1, 22, and 43; 3. Docetaxel (75 mg/m^2) and Cisplatin (80–100 mg/m^2) on days 1, 22, and 43; or 4. Paclitaxel (175 mg/m^2) and Cisplatin (80–100 mg/m^2) on days 1, 22, and 43 during radiation therapy according to the tumor stage and patient's condition.

2.6. Data analysis

All data in the analysis is expressed as the mean ± standard deviation values. Statistical analysis was performed using R software (version 3.5) and $p < 0.05$ (alpha of 0.05) was considered statistically significance. A pairwise two-tailed Student's t test was used to compare the ADC, Dmean, Kmean and FA values for the temporal lobe before and after therapy across time points, and was also used to compare the MoCA score before and after therapy. A chi-square test was used to analyze the number of MoCA <26 participants before and after treatment. A one-way ANOVA was used to determine the significance of neurocognitive impairments in the administered chemotherapy protocols. A *Pearson's* correlation analysis was used to analysis the correlation of DKI parameters and post-CCRT MoCA, and the correlation of delta DKI parameters and ΔMoCA (Δ indicates the change between before treatment and 12 months after CCRT).

3. Results

A total of 56 patients met the inclusion criteria. The clinical information of NPC patients is illustrated in Table 1. The four chemotherapy protocols had no significant effect on neurocognitive impairment ($p = 0.9$). Table 2 provides summary statistics and p-values for parameter comparison. Comparisons are made under the assumption that the signal to noise is consistent across longitudinal study time points.
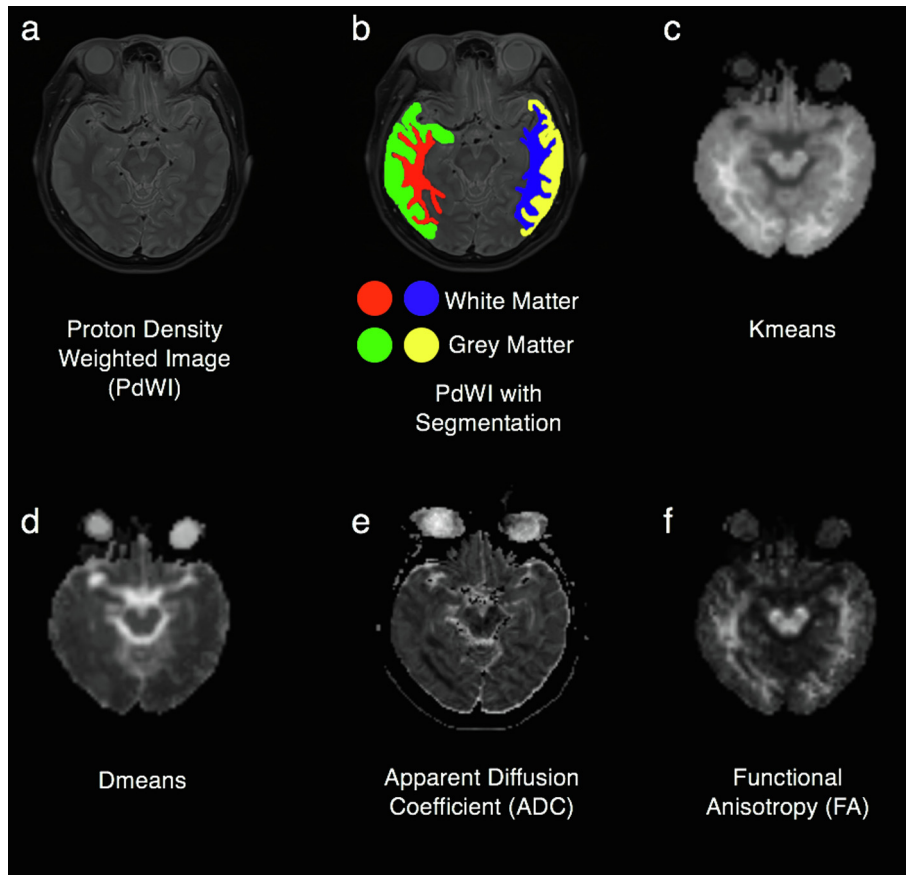
Fig. 2. PdWI without segmentation (a). PdWI with ROIs of the temporal gray and white matter on both sides. (Red shows the right side of the temporal white matter, green shows the right side of the temporal gray matter, blue shows the left side of the temporal white matter, and yellow shows the left side of the temporal grey matter) (b). DKI 4 parametric mapping, including Kmean (c), Dmean (d), ADC (e) and FA (f). (For interpretation of the references to colour in this figure legend, the reader is referred to the web version of this article.)

3.1. Dynamic changes rule of ADC

The longitudinal evolution of ADC values showed that ADC decreased after CCRT, and reached the lowest value at the 3-month time point, then increased. ADC was significantly different compared with baseline at every follow-up time point ($p < 0.05$). Although ADC increased near to baseline value at 12 months after CCRT, it remained significantly lower than at baseline. WM showed more obvious changes in ADC than GM (Fig. 3) (Table 2).

3.2. Dynamic changes of FA and Dmean

Dmean and FA showed a similar temporal pattern as ADC. The Dmean-GM-12 m after CCRT was not different compared to baseline ($p = 0.9$), Dmean and FA at other follow-up time points were significantly different compared with the baseline ($p < 0.05$). Dmean and FA also reached the lowest value three-months after CCRT. The mean FA value of WM was significantly lower than that of GM at all time points ($p < 0.05$) (Fig. 3) (Table 2).

3.3. Dynamic changes of Kmean

Kmean has a vastly different temporal pattern when compared to the other extracted quantitative parameters (Dmean, FA, ADC). Kmean continuously declines after CCRT with no recovery. The Kmean at 12 months after treatment was significantly lower than baseline ($p < 0.001$) (Fig. 3) (Table 2).

3.4. Neurocognitive function test

Twelve months after CCRT, the decline was also ascertained in the MoCA score (MoCA-pre 28.036 ± 0.972; MoCA-post 26.179 ± 1.466; $p < 0.001$). No patient showed neurocognitive impairment before CCRT, while 18 patients (32.14%) scored in the impaired range after 12 months of CCRT (MoCA < 26 as cutoff) ($p < 0.001$). 4 (7.14%) patients MoCA declined more than 3 points after 12 months treatment.

3.5. Correlations between parameters

Significant positive correlations were observed between Kmean-WM-6 m, Kmean-WM-12 m, ΔKmean-WM and MoCA-post (Kmean-WM-6 m & MoCA-post, r = 0.351, $p = 0.008$; Kmean-WM-12 m & MoCA-post r = 0.394, $p = 0.003$; delta Kmean-WM & MoCA-post, r = 0.445, $p = 0.001$) (Fig. 4). No significant positive/negative correlation was observed between delta Kmean, ΔDmean, ΔADC, ΔFA and ΔMoCA score (change between before and 12 months after CCRT, $p > 0.05$) of grey or white matter with the Pearson's correlation test.

4. Discussion

RT is an effective treatment modality to destroy cancerous tissues of NPC, but it may also inevitably damage adjacent healthy tissues, especially the sensitive brain tissue of the temporal lobe. Neural structure can be directly or indirectly injured by radiation.

Table 1
Clinical features of the 56 NPC patients included in the study.

Characteristics	Number of patients	
Age, year (range 19–70 y, 47.07 ± 10.86, median = 48 y)		
å ≤ 50	36/56	64.29%
>50	20/56	35.71%
Gender		
Male	34/56	60.71%
Female	22/56	39.29%
Education, year		
≤9	8/56	14.29%
10–12 y	30/56	53.57%
>12 y	18/56	32.14%
Histology, WHO type		
Undifferentiated non-keratinized carcinoma	51/56	91.11%
Differentiated non-keratinized carcinoma	4/56	0.71%
Differentiated squamous cell carcinoma	1/56	0.18%
Stage		
II	13/56	23.21%
III	23/56	41.07%
IV	20/56	35.71%
IMRT Dose, Gy		
68.2	7/56	12.50%
69.75	21/56	37.50%
70.06	18/56	32.14%
72.1	10/56	17.86%
Chemotherapy		
Cisplatin (30–40 mg/m^2) weekly	8/56	14.29%
Cisplatin (80–100 mg/m^2) on days 1, 22, and 43	6/56	10.71%
Docetaxel (75 mg/m^2) and Cisplatin (80–100 mg/m^2) on days 1, 22, and 43	26/56	46.43%
Paclitaxel (175 mg/m^2) and Cisplatin (80–100 mg/m^2) on days 1, 22, and 43	16/56	28.57%

NPC = nasopharyngeal carcinoma, IMRT = intensity-modulated radiotherapy.

Researchers have made multiple hypotheses on understanding this phenomenon. One theory is that the damage of vascular endothelial cells follows local brain tissue ischemia of the whole brain [26]. Larger scale, nonlocalized injury of the brain may be induced by RT due to central nervous system autoimmune vasculitis [11]. Evaluation of the irradiated temporal microstructural damage at acute reaction and early delayed stages is essential to help with adjusting treatment protocols. Alterations in microstructure and water diffusion within visually normal-appearing temporal lobes shown on conventional MRI can be visualized quantitatively by diffusion technologies, such as DWI, DTI, and DKI. In this study, high-resolution DWI and DKI were both used to detect the micro-injury of normal-appearing temporal lobes at 4 time points over 12 months after CCRT in NPC patients longitudinally.

ADC, FA and Dmean alterations were found to be temporally dynamic and suggestively recover towards values closer to baseline after an initial decline. The greatest decline in these diffusivity parameters occurred at 3-month after CCRT, with subsequent increase between 3 and 12 months. ADC and FA values remained significantly lower at the 12-month after chemoradiotherapy compared with baseline. In future, we plan to evaluate at later time points to determine whether baseline values are fully recoverable. ADC is a classic parameter used to evaluate the water diffusivity of tissue, related to the cellularity, cytotoxic edema, and angiogenic edema [27]. The decline of ADC means restriction of water molecule diffusion. The ADC longitudinal change of normal-appearing temporal lobes after irradiation may have been caused by the transformation period from edema to regression of edema, depending on the unique time-dependent trajectory. However, the ADC was also affected by ischemia derived by vessel injury and myelin microinjury, silenced on the conventional MRI. The mechanism underlying ADC alteration is complex, thus it is challenging to determine the precise sensitivity of this quantity to neuronal injury and restructuring following RT.

Alteration of FA value found in this paper is consistent with previous research by Xiong et. al and Harsan LA et al. [28,29] FA is the most sensitive indicator of the directional anisotropy of water molecules, especially in WM. According to these previous studies, the active hypothesis is that the transient reduction of FA might be attributed to axonal swelling and microinjury of myelin in the acute and early delayed reaction phase. FA progressively increased as a result of an expanded oligodendrocyte population contributed to recovery of myelination and subsequently a mild increase in axonal caliber.

Dmean implies the mean diffusivity and represents a more exact value than ADC as the computation of this parameters allows for the consideration of the three main directions of water movement. Chapman et al. [17] investigated normal appearing white matter in patients with radiation-induced late delayed neurocognitive decline using DTI. Decreases in longitudinal diffusivity ($\lambda \parallel$) and increases in perpendicular diffusivity ($\lambda \perp$) from pre-RT values were observed in the temporal lobe WM at the beginning three weeks after RT. $\lambda \parallel$ quantifies water movement along the main longitudinal direction, evaluating axonal integrity, while $\lambda \perp$ reflects myelin integrity (myelin injury leads to increased $\lambda \perp$). However, Dmean values were not specifically reported in that study. Wang et al. [20] demonstrated that Dmean values were significantly lower one week after RT, but returned to normal in one year, which is consistent with our results. Our results support this finding with further validation through a longitudinal study that can more accurately compare fluctuation in brain microstructuring due to CCRT through utilizing data from the patient's scans prior to treatment as a baseline. This provides this study with a more robust statistical analysis by utilizing the patient's pre-treatment parameters as comparative metrics. Irradiation induces brain tissue injury and vessel injury (alterations in the permeability of the small vessel wall), as a result of edema and consequent demyelination. The transient reduction of Dmean might be attributed to the comprehensive effect of fibrinoid changes to the blood vessels and ischemia. During the recovery period, the increase of Dmean may be caused by the regression of edema and remyelination [30].

Table 2
The summary statistics for parameter comparison.

	Baseline	1 W post CCRT	p value	3 M post CCRT	p value	6 M post CCRT	p value	12 M post CCRT	p value
ADC-WM	686.36 ± 35.60	624.56 ± 39.26	0.000	588.24 ± 38.90	0.000	649.00 ± 36.01	0.000	680.09 ± 36.05	0.006
ADC-GM	850.90 ± 45.95	821.05 ± 42.95	0.000	791.28 ± 45.46	0.000	823.37 ± 43.49	0.000	841.91 ± 51.37	0.001
FA-WM	0.419 ± 0.03	0.389 ± 0.03	0.000	0.365 ± 0.03	0.000	0.368 ± 0.03	0.000	0.401 ± 0.03	0.000
FA-GM	0.190 ± 0.02	0.175 ± 0.02	0.000	0.163 ± 0.02	0.000	0.166 ± 0.02	0.000	0.180 ± 0.02	0.000
Dmean-WM	1.147 ± 0.11	0.931 ± 0.09	0.000	0.778 ± 0.08	0.000	1.008 ± 0.1	0.000	1.180 ± 0.1	0.001
Dmean-GM	1.407 ± 0.21	1.198 ± 0.16	0.000	1.046 ± 0.14	0.000	1.213 ± 0.16	0.000	1.405 ± 0.19	0.9
Kmean-WM	0.764 ± 0.1	0.699 ± 0.09	0.000	0.623 ± 0.09	0.000	0.545 ± 0.08	0.000	0.461 ± 0.08	0.000
Kmean-GM	0.663 ± 0.08	0.649 ± 0.08	0.098	0.571 ± 0.08	0.000	0.477 ± 0.07	0.000	0.395 ± 0.06	0.000

W, week; M, month(s); WM, white matter; GM, gray matter; CCRT, Concurrent Chemoradiotherapy. P value presented that statistics for parameters comparison between every time point with baseline.
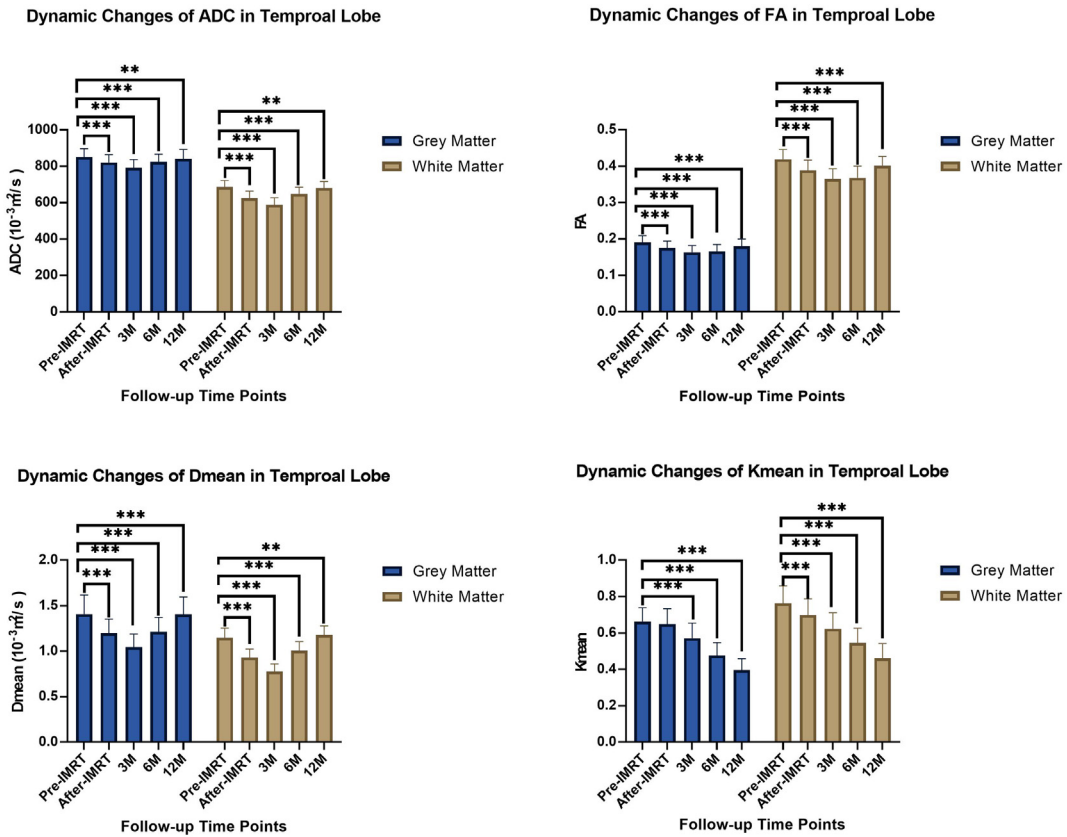
Fig. 3. The column chart showed dynamic changes of DKI parameters of the temporal lobe in NPC patients receiving CCMT.
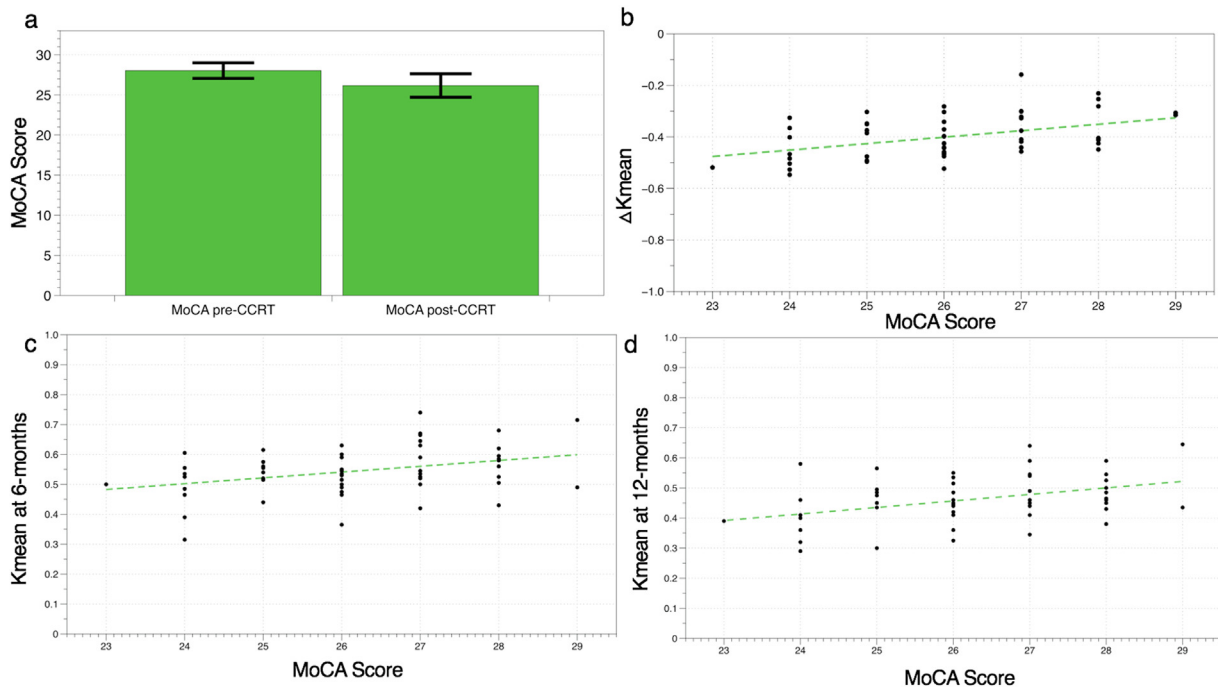

Fig. 4. The column chart showed MoCA score declined twelve months after CCRT (a). Significant positive correlations were observed between ΔKmean-WM (b), Kmean-WM-6 m (c), Kmean-WM-12 m (d) and MoCA-post (delta Kmean-WM & MoCA-post, r = 0.445, p = 0.001; Kmean-WM-6 m & MoCA-post, r = 0.351, p = 0.008; Kmean-WM-12 m & MoCA-post r = 0.394, p = 0.003).

Kmean has a different temporal response than the other parameters. Kmean continued to decline over 12 months after CCRT. Kmean at the 12-month time point was significantly lower than baseline (GM and WM, $p < 0.001$). Wang and colleagues [20] found that gray and white matter Kmean values were significantly higher 1 week after CCRT, but significantly lower at

6-month and 1-year time points. The change of Kmean value at the long time points (6 months and 1 year) showed the same results in our study. However, the short time points have differing results, with statistically significant decrease in Kmeans in our study (GM, $p = 0.98$; WM, $p < 0.001$). The possible reason is that the pathological changes of temporal lobe microstructure in acute reaction phase is complicated and influenced by multiple variables. This includes acute immune response effects, which vary from patient to patient [31]. Further research is needed to verify, with further longitudinal study time points. Given prior studies and our results, we conclude that Kmean is sensitive to microstructural change and structural complexity of tissue. It would seem that Kmeans is a more useful metric for identifying CCRT side effects at further time points, as the acute phase may have considerable heterogeneity in Kmean values dependent on patient derived characteristics of NPC tumor and baseline neurological condition as suggested by this study when compared to other studies. Microstructural damage or increased homogeneity may be the reason for the continuous change of Kmean after RT. The continuous decrease of Kmean over 1 year after IMRT indicated that microstructural destruction, or fibrinoid changes in the blood vessels, induced continuous damage, although edema disappeared and myelin reformed. Different microstructural change present in different period, running through the three phase of irradiation reaction of brain tissue. The acute reaction and early delayed radiation period is characterized by cell or myelin edema, blood brain barrier damage. And the late delayed radiation period is characterized by demyelination, vascular abnormalities, considered as irreversible and progressive [32]. Neurocognitive score progressively declines in the 2 years after chemoradiotherapy supported our results of Kmean from another perspective [7]. Our study supplements the study by Wang et al in that we conclude that it is seemingly important to use both Kmeans along with another parameter to monitor RT induced neurological damage, as Kmeans may be more variable and less reliable in the short term, but more sensitive in the long term. Contrarily, Dmeans, ADC, and FA may be more consistent in the short term and provide the immediate temporal response more reproducibly, however less sensitive and thus failing to show restructuring and changes in the long term.

Traditionally, white matter and vascular endothelium have been regarded as the core brain structures damaged by irradiation [33]. White matter is recognized as the most vulnerable structure in the brain's response to irradiation [34] in clinical evaluation because of myelination. Our results reinforce this tendency, with the parameter sensitivity being higher in white matter analysis than in gray matter analysis. However, many previous studies [17,26,28] only focus on the white matter of the temporal lobe in NPC patients, under the hypothesis that gray matter was not affected by RT. More recently, studies began to evaluate grey matter alterations as well. The volume or the thickness of gray matter, appearing normal on conventional MRI, decreased after RT [11]. Our results showed that the diffusion parameters also revealed changes in grey matter, indicating that gray matter also had microstructural changes induced by irradiation and reinforcing the importance of investigating this in future research.

Twelve months after CCRT, neurocognitive function score (MoCA) declined compared with baseline as is confirmed by many other studies [6,7,35]. The results of this study show positive correlation between parameters Kmean-WM-6 m, Kmean-WM-12 m, delta Kmean-WM and MoCA-post. This is bolstered by previous work [17]. Given these results, it is feasible to conclude that the diffusion-related imaging parameters could be considered as a biomarker related to neurocognitive impairment. However, which parameter is more sensitive at what time point requires more experimental and clinical verification.

From the perspective of deriving more statistically robust comparative parameters, future research will focus on MRI voxel level longitudinal comparisons in order to utilize high resolution imaging to further pinpoint regional microstructural abnormalities within WM and GM tracks. This could provide correlations between RT localization and tissue sensitivity to radiation induced injury. Furthermore, signal to noise will be thoroughly characterized for all imaging time points in the longitudinal study in order to provide a sound statistical comparison for voxel level dynamic change studies.

This study has several limitations. First, the basis of this study is that the diffusion related imaging parameters from MRI have some quantitative significance related to microstructural alterations of tissue. While this is bolstered by previous work, this is still a hypothesis that must be tested from a structural and molecular standpoint, necessitating rigorous biological correlations that are challenging to perform in healthy patients without invasive procedures such as biopsy [11–15]. The precise underlying mechanisms must be elucidated by comparison to biopsied tissue, post-mortem evaluation, other clinical neurocognitive metrics and markers, and in vivo studies. The second limitation is that this study executed an identical dose gradient and radiation field design. Further research into imaging parameter optimization will allow for more robust and sensitive results. Third, although our follow-up time of up to 12 months was relatively long compared with other studies, and the reversibility of these alterations could not be determined. Further longitudinal study is necessitated to assess patients. Finally, all patients underwent CCRT rather than IMRT only, which may cause a chemotherapy-induced effect or synergy between chemotherapy and IMRT, making decoupling effects more challenging for this type of pilot study.

5. Conclusion

This study provides a basis for the use of high-resolution DWI and DKI to detect early radiation-induced microstructural abnormalities that are undetectable by conventional MRI of temporal lobes following chemoradiotherapy in NPC patients. The longitudinal change of Kmean in the results indicates that the microstructural changes in the temporal lobe might exist for longer than predicted by other parameters (Dmean, ADC, FA). In addition to white matter, gray matter also underwent significant microstructural changes as predicted by the parameters obtained from diffusion based MRI after chemoradiotherapy. High-resolution DWI and DKI, combined with neurocognitive testing might be extended as a protocol to detect neurocognitive impairment regularly in NPC and other head and neck cancers.

Declaration of Competing Interest

The authors declare that they have no known competing financial interests or personal relationships that could have appeared to influence the work reported in this paper.

References

[1] Chen J, Dassarath M, Yin ZY, Liu HL, Yang KY, Wu G. Radiation induced temporal lobe necrosis in patients with nasopharyngeal carcinoma: a review of new avenues in its management. Radiat Oncol 2011;6.

[2] Zhou XF, Liao XF, Ren XQ, et al. Dynamic MRI follow-up of radiation encephalopathy in the temporal lobe following nasopharyngeal carcinoma radiotherapy. Oncol Lett 2017;14:715–24.

[3] Mao YP, Zhou GQ, Liu LZ, et al. Comparison of radiological and clinical features of temporal lobe necrosis in nasopharyngeal carcinoma patients treated with 2D radiotherapy or intensity-modulated radiotherapy. Br J Cancer 2014;110:2633–9.

[4] Chen L, Zhang Y, Lai SZ, et al. 10-Year results of therapeutic ratio by intensity-modulated radiotherapy versus two-dimensional radiotherapy in patients with nasopharyngeal carcinoma. Oncologist 2019;24:E38–45.

[5] Wang XC, Zhang XD, Dong L, Liu H, Wu QW, Mohan R. Development of methods for beam angle optimization for IMRT using an accelerated exhaustive search strategy. Int J Radiat Oncol Biol Phys 2004;60:1325–37.

[6] McDowell LJ, Ringash J, Xu W, et al. A cross sectional study in cognitive and neurobehavioral impairment in long-term nasopharyngeal cancer survivors treated with intensity-modulated radiotherapy. Radiother Oncol 2019;131:179–85.

[7] Zer A, Pond GR, Razak ARA, et al. Association of neurocognitive deficits with radiotherapy or chemoradiotherapy for patients with head and neck cancer. JAMA Otolaryngol Head Neck Surg 2018;144:71–9.

[8] Bolt S, Eadie T, Yorkston K, Baylor C, Amtmann D. Variables associated with communicative participation after head and neck cancer. JAMA Otolaryngol Head Neck Surg 2016;142:1145–51.

[9] Bernstein LJ, Pond GR, Gan HK, et al. Pretreatment neurocognitive function and self-reported symptoms in patients with newly diagnosed head and neck cancer compared with noncancer cohort. Head Neck 2018;40:2029–42.

[10] Guo Z, Han LJ, Yang YD, et al. Longitudinal brain structural alterations in patients with nasopharyngeal carcinoma early after radiotherapy. Neuroimage-Clin 2018;19:252–9.

[11] Lin JB, Lv XF, Niu MQ, et al. Radiation-induced abnormal cortical thickness in patients with nasopharyngeal carcinoma after radiotherapy. Neuroimage-Clin 2017;14:610–21.

[12] Lv XF, Zheng XL, Zhang WD, et al. Radiation-induced changes in normal-appearing gray matter in patients with nasopharyngeal carcinoma: a magnetic resonance imaging voxel-based morphometry study. Neuroradiology 2014;56:423–30.

[13] Wang HZ, Qiu SJ, Lv XF, et al. Diffusion tensor imaging and H-1-MRS study on radiation-induced brain injury after nasopharyngeal carcinoma radiotherapy. Clin Radiol 2012;67:340–5.

[14] Munter MW, Karger CP, Schneider HM, Peschke P, Debus J. Delayed vascular injury after single high-dose irradiation in the rat brain: Histologic, immunohistochemical, and angiographic studies. Radiology 1999;212:475–82.

[15] Evangelou N, Esiri MM, Smith S, Palace J, Matthews PM. Quantitative pathological evidence for axonal loss in normal appearing white matter in multiple sclerosis. Ann Neurol 2000;47:391–5.

[16] Viallon M, Cuvinciuc V, Delattre B, et al. State-of-the-art MRI techniques in neuroradiology: principles, pitfalls, and clinical applications. Neuroradiology 2015;57:441–67.

[17] Chapman CH, Nagesh V, Sundgren PC, et al. Diffusion tensor imaging of normal-appearing white matter as biomarker for radiation-induced late delayed cognitive decline. Int J Radiat Oncol Biol Phys 2012;82:2033–40.

[18] Chen WS, Qiu SJ, Li JJ, et al. Diffusion tensor imaging study on radiation-induced brain injury in nasopharyngeal carcinoma during and after radiotherapy. Tumori 2015;101:487–90.

[19] Lu LY, Wang S, Wang Q, et al. Diffusion kurtosis as an in vivo imaging marker of early radiation-induced changes in radiation-induced temporal lobe necrosis in nasopharyngeal carcinoma patients. Clin Neuroradiol 2018;28:413–20.

[20] Wang D, Li YH, Fu J, Wang H. Diffusion kurtosis imaging study on temporal lobe after nasopharyngeal carcinoma radiotherapy. Brain Res 2016;1648:387–93.

[21] Tabesh A, Jensen JH, Ardekani BA, Helpern JA. Estimation of tensors and tensor-derived measures in diffusional kurtosis imaging (vol 65, pg 823, 2011). Magn Reson Med 2011;65. 1507-1507.

[22] Yushkevich PA, Piven J, Hazlett HC, et al. User-guided 3D active contour segmentation of anatomical structures: significantly improved efficiency and reliability. Neuroimage 2006;31:1116–28.

[23] Nasreddine ZS, Phillips NA, Bédirian V, et al. The Montreal Cognitive Assessment, MoCA: a brief screening tool for mild cognitive impairment. J Am Geriatr Soc 2005;53:695–9.

[24] Gómez F, Zunzunegui M, Lord C, Alvarado B, García A. Applicability of the MoCA-S test in populations with little education in Colombia. Int J Geriatr Psychiatry 2013;28:813–20.

[25] Monica WKK, Lucullus HTL, Peter KNY. The use of biologically related model (Eclipse) for the intensity-modulated radiation therapy planning of nasopharyngeal carcinomas. PLoS One 2014;9:e112229.

[26] Duan FH, Cheng JL, Jiang JW, Chang J, Zhang Y, Qiu SJ. Whole-brain changes in white matter microstructure after radiotherapy for nasopharyngeal carcinoma: a diffusion tensor imaging study. Eur Arch Otorhinolaryngol 2016;273:4453–9.

[27] Drake-Perez M, Boto J, Fitsiori A, Lovblad K, Vargas MI. Clinical applications of diffusion weighted imaging in neuroradiology. Insights into Imaging 2018;9:535–47.

[28] Xiong WF, Qiu SJ, Wang HZ, Lv XF. 1H-MR spectroscopy and diffusion tensor imaging of normal-appearing temporal white matter in patients with nasopharyngeal carcinoma after irradiation: initial experience. J Magn Reson Imaging 2013;37:101–8.

[29] Harsan LA, Poulet P, Guignard B, et al. Brain dysmyelination and recovery assessment by noninvasive in vivo diffusion tensor magnetic resonance imaging. J Neurosci Res 2006;83:392–402.

[30] Garsa A, Ho JC, Hu C, Chang EL. Bevacizumab is more effective in nasopharyngeal carcinoma patients with lower maximum radiation dose to the temporal lobe. Chin Clin Oncol 2019.

[31] Nieder C, Andratschke N, Astner ST. Experimental concepts for toxicity prevention and tissue restoration after central nervous system irradiation. Radiat Oncol 2007;2:23.

[32] Lee YW, Cho HJ, Lee WH, Sonntag WE. Whole brain radiation-induced cognitive impairment: pathophysiological mechanisms and therapeutic targets. Biomol Ther 2012;20:357–70.

[33] Andrews RN, Metheny-Barlow LJ, Peiffer AM, et al. Cerebrovascular remodeling and neuroinflammation is a late effect of radiation-induced brain injury in non-human primates. Radiat Res 2017;187:599–611.

[34] Lee AWM, Ng SH, Ho JHC, et al. Clinical-diagnosis of late temporal-lobe necrosis following radiation-therapy for nasopharyngeal carcinoma. Cancer 1988;61:1535–42.

[35] Welsh LC, Dunlop AW, McGovern T, et al. Neurocognitive function after (chemo)-radiotherapy for head and neck cancer. Clin Oncol 2014;26:765–75.